

Kinetics and Thermodynamics of Hydrogen Atom Transfer to Superoxometal Complexes

Andreja Bakac

Contribution from Ames Laboratory, Iowa State University, Ames, Iowa 50011

Received June 16, 1997[⊗]

Abstract: Dicationic metal superoxo complexes, $L(H_2O)MOO^{2+}$ ($M = Rh, Cr; L = (NH_3)_4, (H_2O)_5, [14]aneN_4$) react with rhodium hydrides $L'(H_2O)RhH^{2+}$ ($L' = (NH_3)_4, [14]aneN_4$, and *meso*- $Me_6-[14]aneN_4$) to yield $L(H_2O)MOOH^{2+}$ and $L'(H_2O)_2Rh^{2+}$. The rhodium(II) product is rapidly converted to $L'(H_2O)RhOO^{2+}$ in a reaction with molecular oxygen ($k \sim 10^8 M^{-1} s^{-1}$), or to a binuclear superoxo product in the absence of O_2 . When the central metal atom and nonparticipating ligands are identical in the two reactants ($M = Rh, L = L'$), the O_2 insertion into $Rh-H$ bond becomes catalytic, $L'RhH^{2+} + O_2 \rightarrow L'RhOOH^{2+}$ ($L'RhOO^{2+} = \text{catalyst}$). The hydrogen transfer step exhibits a large kinetic isotope effect ($k_H/k_D = 7.6$ for the reaction of $Cr_{aq}OO^{2+}$ with $([14]aneN_4)(H_2O)RhH^{2+}$, $\Delta H_H^\ddagger = 20.3 \pm 1.8 \text{ kJ mol}^{-1}$, $\Delta S_H^\ddagger = -136 \pm 6 \text{ J mol}^{-1} K^{-1}$, and $\Delta H_D^\ddagger = 24.7 \pm 4.3 \text{ kJ mol}^{-1}$, $\Delta S_D^\ddagger = -138 \pm 15 \text{ J mol}^{-1} K^{-1}$), but the isotopic composition of the solvent has no effect on rates, $k_{H_2O}/k_{D_2O} = 1$. Steric effects play a major role in the kinetics. From the available thermochemical data, the energy of the $Cr_{aq}OO-H^{2+}$ bond was calculated to be $\sim 330 \text{ kJ/mol}$.

Introduction

Autoxidation of hydrocarbons to (initially) alkyl hydroperoxides is one of the most thoroughly investigated radical chain reactions.^{1–5} In the propagating steps, eqs 1 and 2,



alkylperoxyl radicals abstract a hydrogen atom from the hydrocarbon yielding carbon-centered radicals and the hydroperoxide. Alkyl radicals are captured by O_2 to regenerate alkylperoxyl radicals and continue the chain.

A number of transition metal complexes catalyze the autoxidation of organic materials. The key catalytic intermediates are either high-valent metals or organic radicals.^{2,5} Metal ions often react with the initially formed hydroperoxides to generate radicals which perpetuate the chain.^{1–7} Superoxometal compounds may also be involved as short-lived precursors to radical intermediates. For example, alkyl and alkylperoxyl radicals may be formed by the hydrogen atom transfer of eq 3 ($L = \text{ligand}$



system, $M = \text{metal}$), followed by reaction 2.^{4,8–12} Obviously,

[⊗] Abstract published in *Advance ACS Abstracts*, October 15, 1997.

(1) Simandi, L. I. *Catalytic Activation of Dioxygen by Metal Complexes*; Kluwer Academic Publishers: Dordrecht/Boston/London, 1992.

(2) Sheldon, R. A. In *The Activation of Dioxygen and Homogeneous Catalytic Oxidation*; Barton, D. H. R., Martell, A. E., Sawyer, D. T., Eds.; Plenum: New York and London, 1993; pp 9–30.

(3) Parshall, G. W.; Ittel, S. D. *Homogeneous Catalysis*, 2nd ed.; Wiley: New York, 1992; Chapter 10.

(4) Sheldon, R.; Kochi, J. K. *Adv. Catal.* **1976**, *25*, 272.

(5) Shilov, A. E. *Activation of Saturated Hydrocarbons by Transition Metal Complexes*, D. Reidel Publishing Co.: Dordrecht, The Netherlands, 1984; Chapter 4.

(6) Bottcher, A.; Birnbaum, E. R.; Day, M. W.; Gray, H. B.; Grinstaff, M. W.; Labinger, J. A. *J. Mol. Catal.* **1997**, *117*, 229.

(7) Franz, G.; Sheldon, R. A. in *Ullmann's Encyclopedia of Industrial Chemistry*; VCH: Weinheim, Germany, 1991; pp 261–311.

(8) Bailey, C. L.; Drago, R. S. *Coord. Chem. Rev.* **1987**, *79*, 321.

(9) Nishinaga, A.; Yamato, H.; Abe, T.; Maruyama, K.; Matsuura, T. *Tetrahedron Lett.* **1988**, *29*, 6309.

this mechanism is limited to compounds with relatively weak C–H bonds, which rules out most of nonfunctionalized alkanes. The enzyme-catalyzed oxidation of these and other materials in biological environments often involves superoxometal intermediates but only as precursors to more potent oxidizing species and not as hydrogen atom abstracting agents.^{13–15}

In support of reaction 3, several superoxometal complexes have been shown to oxidize compounds with moderately weak C–H bonds, such as cumene, phenols, alcohols, and amines.^{16–18} Later studies have shown, however, that mechanisms other than hydrogen atom abstraction can rationalize the results equally well or better.² For example, the autoxidation of cumene and cyclohexene is now believed to be initiated by metal-catalyzed decomposition of trace amounts of alkyl hydroperoxides, and the oxidation of phenols catalyzed by cobalt and manganese Schiff-base complexes involves peroxide displacement from superoxo or peroxy metal complexes, eq 4, followed by cobalt–oxygen bond homolysis and the reaction of phenoxyl radicals with O_2 .²



Hydrogen transfer thus appears to be a low-probability pathway for superoxometal complexes, at least in the cases examined. From the limited number of mechanistic studies^{2,16–18} it is not clear whether the observed behavior is determined by the kinetics or thermodynamics. Moreover, the energy of the O–H bonds in $LMOOH^n$ and even the exact chemical composition of the superoxo and hydroperoxy species in catalytic oxygenation reactions are usually not known.

(10) Nishinaga, A.; Tomita, H. *J. Mol. Catal.* **1980**, *7*, 179.

(11) Stern, E. W. *Chem. Commun.* **1970**, 736.

(12) Kropf, H.; Knaack, K. *Tetrahedron* **1972**, *28*, 1143.

(13) Guengerich, F. P. *Am. Sci.* **1993**, *81*, 440.

(14) Verkhovskiy, M. I.; Morgan, J. E.; Wikstrom, M. *Biochemistry* **1994**, *33*, 3079.

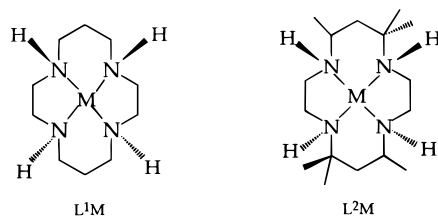
(15) Feig, A. L.; Lippard, S. J. *Chem. Rev.* **1994**, *94*, 759.

(16) Abel, E. W.; Pratt, J. M.; Whelan, R.; Wilkinson, P. J. *J. Am. Chem. Soc.* **1974**, *96*, 7119.

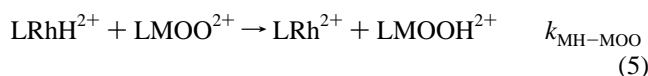
(17) Ghosh, S. P.; Gelerinter, E.; Pyrka, G.; Gould, E. S. *Inorg. Chem.* **1993**, *32*, 4780.

(18) Bear, J. L.; Yao, C.-L.; Capdevielle, F. J.; Kadish, K. M. *Inorg. Chem.* **1988**, *27*, 3782.

Chart 1



Whether or not LMOO^n complexes engage in hydrogen atom transfer is an important mechanistic question in the area of catalytic autoxidation. We decided to address this issue by examining several cases with favorable thermodynamics. Rhodium(III) hydrides were chosen as hydrogen donors, and the expected chemistry is shown in eq 5. The rapid capture of



LRh^{2+} by molecular oxygen in the next rapid step should yield the superoxorhodium complexes LRhOO^{2+} , eq 6. The reactants in eq 5 are well-defined species, as are the expected metal hydroperoxo and rhodium superoxo products.^{19–22} Hydrogen atom transfer between $(\text{NH}_3)_4(\text{H}_2\text{O})\text{RhH}^{2+}$ and $(\text{NH}_3)_4(\text{H}_2\text{O})\text{RhOO}^{2+}$ has been implied as a step in photochemical O_2 insertion into a Rh-H bond,²¹ but no direct evidence for this step was presented.

Although the LRh-H and LMOO-H bond dissociation energies (BDE) have not been determined for the complexes used in this work, reaction 5 is believed to be thermodynamically favored given that Rh-H bonds are generally weaker than O-H bonds; see Discussion. Also, other reaction pathways, such as peroxy displacement, would require an unlikely metal-metal-bonded complex to be formed in a reaction analogous to that in eq 4. Importantly, all the superoxo complexes and rhodium hydrides in this work can be handled under both aerobic and anaerobic conditions in dilute aqueous acid. The ability to work with LMOO^{2+} in the absence of O_2 and with LMH^{2+} in the presence of O_2 provides a great opportunity to examine the nature and role of intermediates over a range of conditions and establish the mechanism with some confidence.

Experimental Section

The complexes *cis*- and *trans*- $[\text{L}^1\text{RhCl}_2]\text{Cl}$, *trans*- $[\text{L}^2\text{RhCl}_2]\text{Cl}$, *trans*- $[\text{L}^1\text{RhH}](\text{ZnCl}_4)$, $[(\text{NH}_3)_5\text{RhH}](\text{SO}_4)$, and *trans*- $[(\text{NH}_3)_4(\text{H}_2\text{O})\text{RhH}](\text{SO}_4)$ were prepared as solids by published procedures,^{20,23–25} and the novel *trans*- $[\text{L}^2(\text{Cl})\text{RhH}](\text{ZnCl}_4)_{0.5}$ by a procedure analogous to that used for the L^1 complex (Chart 1).²⁰ (Data for $[\text{L}^2(\text{Cl})\text{RhH}](\text{ZnCl}_4)_{0.5}$ are as follows. NMR (in dms_o-d_6): -20.14 ppm ($J_{\text{Rh-H}} = 30$ Hz). Ligand methyl groups appear at 1.09 ppm (unresolved, 6 H), 1.16 (s, 3H), 1.20 (s, 3 H), 1.22 (s, 3H) 1.39 (s, 3H). IR (powder): $\nu_{\text{Rh-H}} 2123$ cm^{-1}). The solid *trans*- $[(\text{NH}_3)_4(\text{H}_2\text{O})\text{RhH}](\text{ClO}_4)_2$ was prepared by dissolving 0.25 g of $[(\text{NH}_3)_5\text{RhH}](\text{SO}_4)$ ²⁴ in 7.5 mL of H_2O containing 0.25 mL of 28% NH_3 at 45 °C under Ar and adding 7.5 mL of saturated aqueous solution of NaClO_4 . The suspension was cooled to room temperature and filtered. The solid was washed with acetone and

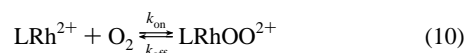
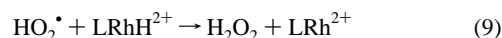
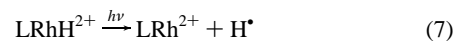
redissolved in H_2O , and the procedure was repeated one more time. The UV-visible spectrum of the final product was identical to that of the chloride salt.²⁴

Caution! Perchlorate salts of transition metal complexes are potentially explosive. Preparations should be carried out on small scales only, and such materials should be handled with care.

Solutions of *cis*- and *trans*- $\text{L}^1(\text{H}_2\text{O})\text{RhH}^{2+}$, *trans*- $(\text{NH}_3)_4(\text{H}_2\text{O})\text{RhH}^{2+}$, and β -*trans*-(*meso*- L^2)($\text{H}_2\text{O})\text{RhH}^{2+}$ (hereafter $\text{L}^1\text{RhH}^{2+}$, $(\text{NH}_3)_4\text{RhH}^{2+}$, and $\text{L}^2\text{RhH}^{2+}$, respectively) in dilute trifluoromethanesulfonic or perchloric acid were prepared by ion exchange of the chloride or sulfate salts, as described previously.²⁰ Some solutions of *trans*- $(\text{NH}_3)_4\text{RhH}^{2+}$ were obtained by dissolution of the solid perchlorate salt without ion-exchange. The deuterated complex *trans*- $\text{L}^1(\text{D}_2\text{O})\text{RhD}^{2+}$ was prepared and stored in $\text{DClO}_4/\text{D}_2\text{O}$ (>95% D). Solutions of the macrocyclic rhodium hydrides survived for several days under argon at 0 °C and several months in a freezer. The tetraammine complex decomposes more readily, and fresh solutions were prepared frequently.

Dilute solutions of $\text{L}^1\text{CrOO}^{2+}$ and $\text{Cr}_{\text{aq}}\text{OO}^{2+}$ were prepared at 0 °C from the chromium(II) precursors and an excess of molecular oxygen.^{19,26} For kinetic purposes, fresh stock solutions of $\text{L}^1\text{CrOO}^{2+}$ were prepared daily. Solutions of $\text{Cr}_{\text{aq}}\text{OO}^{2+}$ generate chromate on standing.²⁷ To avoid complications from the rhodium hydride-chromate reaction, a fresh solution of $\text{Cr}_{\text{aq}}\text{OO}^{2+}$ was prepared for each kinetic run.

Solutions of *trans*- $\text{L}^1\text{RhOO}^{2+}$, *cis*- $\text{L}^1\text{RhOO}^{2+}$, $\text{L}^2\text{RhOO}^{2+}$, and $(\text{NH}_3)_4\text{RhOO}^{2+}$ were prepared by UV-photolysis (Rayonet reactor) of the corresponding rhodium hydrides in O_2 -saturated solutions. Under typical conditions, a 60-s photolysis of 0.2 mM rhodium hydride produced ~ 0.08 mM superoxorhodium complex. Because the products absorb in the UV much more intensely than the reactants do, further photolysis had little effect on product yields. The chemistry during photolysis is believed to take place as in eqs 7–10^{20,21} (L = ligand system) so that the photolyzed solutions contain some H_2O_2 and



unreacted rhodium hydride in addition to the desired superoxo complex. These unavoidable impurities did not seem to interfere with subsequent chemistry. Deliberate addition of 0.1 mM H_2O_2 had no effect on the products or kinetics of any of the reactions studied in this work.

The molar absorptivity (ϵ) of *trans*- $\text{L}^1\text{RhOO}^{2+}$ at 267 nm was determined by spectrophotometric titrations with $\text{Ru}(\text{NH}_3)_6^{2+}$ under air-free conditions and assuming a 1:1 stoichiometry ($\text{L}^1\text{RhOO}^{2+} + \text{Ru}(\text{NH}_3)_6^{2+} + \text{H}^+ \rightarrow \text{L}^1\text{RhOOH}^{2+} + \text{Ru}(\text{NH}_3)_6^{3+}$). Similar titrations were also conducted with $\text{Fe}_{\text{aq}}^{2+}$ under both aerobic and anaerobic conditions. These experiments yielded $\epsilon = (9 \pm 1) \times 10^3 \text{ M}^{-1} \text{ cm}^{-1}$, similar to the values for other superoxorhodium complexes with saturated amine ligands^{22,28} and somewhat larger than our previous estimate of $(5.5 \pm 1.5) \times 10^3 \text{ M}^{-1} \text{ cm}^{-1}$.²⁰

The kinetics of hydrogen transfer were monitored at the UV-maxima of LRhOOH^{2+} ($\lambda 240$ nm, $\epsilon = 4025 \text{ M}^{-1} \text{ cm}^{-1}$ for $(\text{NH}_3)_4\text{RhOOH}^{2+}$ ²¹ and $\epsilon \sim 4000$ for *trans*- $\text{L}^1\text{RhOOH}^{2+}$) or LRhOO^{2+} ($\lambda 270$, $\epsilon = 9600 \text{ M}^{-1} \text{ cm}^{-1}$ for $(\text{NH}_3)_4\text{RhOO}^{2+}$ ²² and $\epsilon = 9000$ for *trans*- $\text{L}^1\text{RhOO}^{2+}$; see above). Experiments were carried out under pseudo-first-order conditions using LRhH^{2+} in ≥ 10 -fold excess over the superoxometal complexes (LRhOO^{2+} , $\text{Cr}_{\text{aq}}\text{OO}^{2+}$, or $\text{L}^1\text{CrOO}^{2+}$), which were kept at the 0.02–0.1 mM level. Ionic strength was kept constant at 0.10 M ($\text{CF}_3\text{SO}_3\text{H}/\text{CF}_3\text{SO}_3\text{Li}$ or $\text{HClO}_4/\text{LiClO}_4$). The nature of the anion (triflate *vs* perchlorate) had no effect on reaction rates. For experiments using LRhOO^{2+} complexes under anaerobic conditions, the superoxo complex was first prepared in an O_2 -saturated solution, allowed to stand

(26) Bakac, A.; Scott, S. L.; Espenson, J. H.; Rodgers, K. L. *J. Am. Chem. Soc.* **1995**, *117*, 6483.

(27) Bakac, A.; Won, T. J.; Espenson, J. H. *Inorg. Chem.* **1996**, *35*, 2171.

(28) Gillard, R. D.; Pedrosa de Jesus, J. D. *J. Chem. Soc., Dalton Trans.* **1984**, 1895.

(19) Bakac, A. *Prog. Inorg. Chem.* **1995**, *43*, 267.

(20) Bakac, A.; Thomas, L. M. *Inorg. Chem.* **1996**, *35*, 5880.

(21) Endicott, J. F.; Wong, C.-L.; Inoue, T.; Natarajan, P. *Inorg. Chem.* **1979**, *18*, 450.

(22) Lilie, J.; Simic, M. G.; Endicott, J. F. *Inorg. Chem.* **1975**, *14*, 2129.

(23) Bounsall, E. J.; Koprich, S. R. *Can. J. Chem.* **1970**, *48*, 1481.

(24) Thomas, K.; Osborn, J. A.; Powell, A. R.; Wilkinson, G. *J. Chem. Soc. (A)* **1968**, 1801.

(25) Curtis, N. F.; Cook, D. F. *J. Chem. Soc., Dalton Trans.* **1972**, 691.

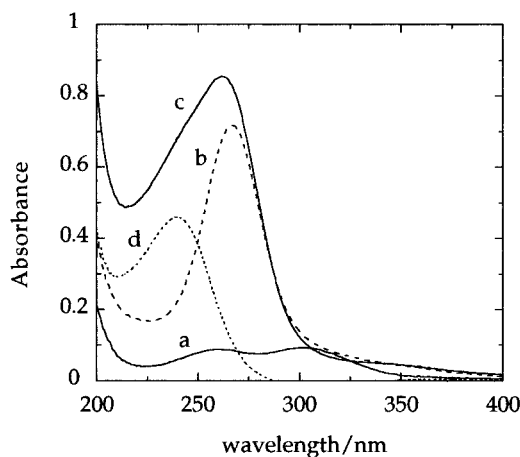


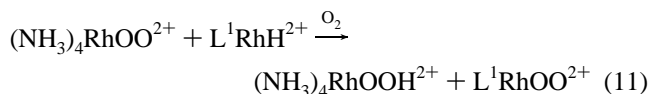
Figure 1. Spectral transformations during the reaction between $(\text{NH}_3)_4\text{RhH}^{2+}$ and $(\text{NH}_3)_4\text{RhOO}^{2+}$ in 4 mM HClO_4 (ionic strength not adjusted): (a) 0.29 mM $(\text{NH}_3)_4\text{RhH}^{2+}$; (b) mixture of $(\text{NH}_3)_4\text{RhOO}^{2+}$ (0.08 mM) and unreacted $(\text{NH}_3)_4\text{RhH}^{2+}$ obtained by partial photolysis of (a) in O_2 saturated solution; (c) after completion of the reaction, eq 14 (2 h); (d) difference between (c) and (b) identifies $(\text{NH}_3)_4\text{RhOOH}^{2+}$ (λ_{max} 240 nm) as reaction product.

until all the remaining LRhH^{2+} was converted to LRhOOH^{2+} , and only then degassed. If the hydride is present during the degassing, the LRhOO^{2+} decomposes readily. The chemistry responsible for this behavior is described later in the section on air-free kinetics.

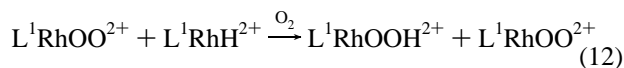
The kinetics of the reaction of *trans*- L^1Rh^{2+} with O_2 were determined by laser flash photolysis utilizing a Nd:YAG laser system described previously.²⁰ All the experiments used λ_{irr} 266 nm. Spectral and most of the kinetic data were collected by use of a Shimadzu 3100 PC spectrophotometer. IR spectra were recorded with a Bio-Rad Digilab FTS-60A FT-IR spectrometer equipped with an MTEC Model 200 photoacoustic cell, and NMR spectra with a Bruker 400 spectrometer.

Results

General Observations. Superoxo- and hydridorhodium complexes react with each other in O_2 - or air-saturated acidic aqueous solutions to form the respective hydroperoxo and superoxo products which were identified and quantified by UV spectroscopy, as shown in Figure 1 for the tetraammine complexes. The reactions are stoichiometric for reactants with different ligand systems, eq 11, but become catalytic if the two



reactants have an identical set of nonparticipating ligands. Reaction 12, for example, represents $\text{L}^1\text{RhOO}^{2+}$ -catalyzed insertion of dioxygen into a Rh–H bond.



Clearly, even the stoichiometric reactions are not free of catalytic effects, because the superoxo products (e.g. $\text{L}^1\text{RhOO}^{2+}$ in eq 11) react further with excess rhodium hydride, as in eq 12. The interference by catalysis in kinetic experiments was minimized by proper choice of reaction conditions and monitoring wavelength, as described below for individual cases.

Rhodium hydrides react also with superoxo complexes of other metals. For example, $\text{Cr}_{\text{aq}}\text{OO}^{2+}$ is reduced to $\text{Cr}_{\text{aq}}\text{OOH}^{2+}$, eq 13. The changes in UV–visible spectra clearly showed the

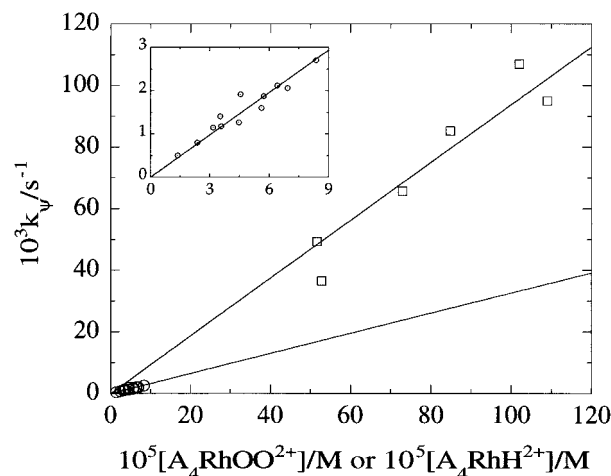
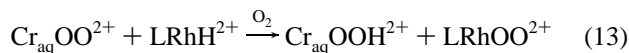
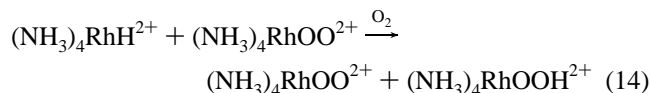


Figure 2. Plot of k_{ψ} against the concentration of the catalyst $(\text{NH}_3)_4\text{RhOO}^{2+}$ for the reaction between $(\text{NH}_3)_4\text{RhH}^{2+}$ and O_2 (circles) and against excess reagent, $(\text{NH}_3)_4\text{RhH}^{2+}$, for the stoichiometric reaction between $(\text{NH}_3)_4\text{RhH}^{2+}$ and $(\text{NH}_3)_4\text{RhOO}^{2+}$ under Ar (squares). The expanded plot for the catalytic reaction is shown as inset. Axis labels for main figure and inset are identical. The four ammonia ligands are abbreviated as A_4 .

disappearance of $\text{Cr}_{\text{aq}}\text{OO}^{2+}$ and the formation of $\text{L}^1\text{RhOO}^{2+}$. The other product, $\text{Cr}_{\text{aq}}\text{OOH}^{2+}$, has no distinct spectral features, Figure S1,²⁹ but its formation was inferred from the overall stoichiometry ($[\text{LRhOO}^{2+}]_{\infty}/[\text{Cr}_{\text{aq}}\text{OO}^{2+}]_0 = 0.9 \pm 0.1$) and by analogy to the related superoxorhodium/hydridorhodium reactions of eqs 11 and 12, where the hydroperoxo products have been identified unambiguously.

Catalytic Reactions. The kinetics were followed by observing the formation of hydroperoxo products in the presence of excess O_2 at 240 nm. The reaction of tetraammine complexes, eq 14, obeyed the mixed second-order rate law of eq 15. At a



$$\frac{d[(\text{NH}_3)_4\text{RhOOH}^{2+}]}{dt} = k_{14}[(\text{NH}_3)_4\text{RhOO}^{2+}][(\text{NH}_3)_4\text{RhH}^{2+}] \quad (15)$$

constant ionic strength of 0.1 M, the rate was independent of $[\text{H}^+]$ (0.003–0.1 M) and $[\text{O}_2]$ (0.20–1.2 mM). A plot of pseudo-first-order rate constants against the concentration of the catalyst $(\text{NH}_3)_4\text{RhOO}^{2+}$, Figure 2, yielded $k_{14} = 32.7 \pm 1.1 \text{ M}^{-1} \text{ s}^{-1}$.

The analogous reaction between *trans*- $\text{L}^1\text{RhH}^{2+}$ and *trans*- $\text{L}^1\text{RhOO}^{2+}$, eq 12, is much slower, and the kinetics were complicated by the decomposition of the product $\text{L}^1\text{RhOOH}^{2+}$ at longer times. The rate constant for reaction 12, $k = 0.4 \text{ M}^{-1} \text{ s}^{-1}$, was determined in a single experiment ($[\text{L}^1\text{RhH}^{2+}]_0 = 0.37 \text{ mM}$, $[\text{L}^1\text{RhOO}^{2+}]_0 = 0.078 \text{ mM}$) from initial rates, assuming a mixed second-order rate law. Under similar conditions, $\text{L}^1\text{RhD}^{2+}$ yielded $k = 0.06 \text{ M}^{-1} \text{ s}^{-1}$. From the two values one calculates a kinetic isotope effect of ~ 7 .

Stoichiometric Reactions. The formation of LRhOO^{2+} in the reactions between $\text{Cr}_{\text{aq}}\text{OO}^{2+}$ and LRhH^{2+} ($\text{L} = (\text{NH}_3)_4$, L^1 , or L^2), eq 13, was monitored at 270 nm. All the reactions obeyed a mixed second-order rate law, eq 16, where $k_{13} = 135$

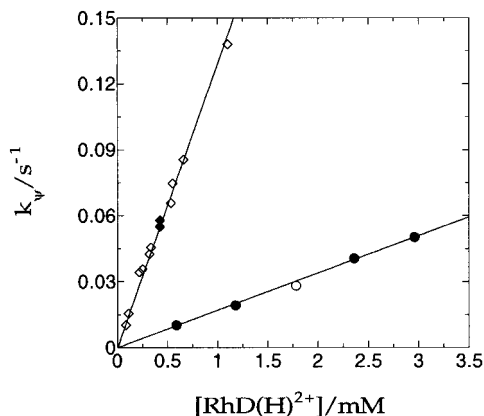
$$\frac{d[\text{LRhOO}^{2+}]}{dt} = k_{13}[\text{Cr}_{\text{aq}}\text{OO}^{2+}][\text{LRhH}^{2+}] \quad (16)$$

$\pm 5 \text{ M}^{-1} \text{ s}^{-1}$ for $(\text{NH}_3)_4\text{RhH}^{2+}$, $129 \pm 3 \text{ M}^{-1} \text{ s}^{-1}$ for *trans*-

Table 1. Rate Constants ($M^{-1} s^{-1}$) for Hydrogen Atom Transfer from Rhodium Hydrides to Superoxometal Complexes^{a-c}

	$Cr_{aq}OO^{2+}$	$(NH_3)_4RhOO^{2+}$	$t-L^1RhOO^{2+}$	$t-L^1CrOO^{2+}$
$(NH_3)_4RhH^{2+}$	135(5)	32.7(11)	93.8(44) ^d	27.6(8) ^d
$t-L^1RhH^{2+}$ ^f	129(3) (25 °C)	22.8(12)	0.4 ^e	<1 ^e
	109(1) (17.5 °C)			
	84.2(34) (11.8 °C)			
	71.6(21) (7.9 °C)			
	63.1(1) (2.4 °C)			
$t-L^1RhD^{2+}$ ^g	17.0(1) (25 °C)		0.06 ^e	
	15.2 ^e (18.1 °C)			
	13.4 ^e (17.5 °C)			
	9.80(10) (11.5 °C)			
	7.59(78) (4.4 °C)			
$c-L^1RhH^{2+}$	123(1)			
$t-L^2RhH^{2+}$	24.1(4)			

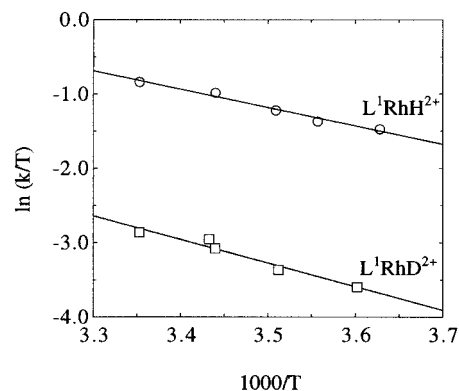
^a In acidic aqueous solutions at 25 °C (unless stated otherwise) and 0.1 M ionic strength. $L^1 = [14]-aneN_4$, $L^2 = meso-Me_6-[14]aneN_4$, $t = trans$, $c = cis$. ^b O_2 atmosphere. ^c Numbers in parentheses represent one standard deviation of the last significant figure. ^d Ar atmosphere. ^e Single measurement. ^f $\Delta H_H^\ddagger = 20.3 \pm 1.8$ kJ/mol, $\Delta S_H^\ddagger = -136 \pm 6$ J/mol K. ^g $\Delta H_D^\ddagger = 24.7 \pm 4.3$ kJ/mol, $\Delta S_D^\ddagger = -138 \pm 15$ J/mol K.

**Figure 3.** Plot of pseudo-first-order rate constants against concentration of rhodium hydrides for the reactions of $Cr_{aq}OO^{2+}$ with L^1RhH^{2+} in H_2O (open diamonds) and in D_2O (filled diamonds) and with L^1RhD^{2+} in H_2O (open circles) and in D_2O (filled circles).

L^1RhH^{2+} , 123 ± 1 $M^{-1} s^{-1}$ for $cis-L^1RhH^{2+}$, and 24.1 ± 0.4 for L^2RhH^{2+} , Table 1. The deuterated complex $trans-L^1RhD^{2+}$ reacts more slowly ($k = 17.0 \pm 0.1$ $M^{-1} s^{-1}$) than its protiated analog, resulting in a deuterium kinetic isotope effect of 7.6 at 25 °C. The rate constants for both $trans-L^1RhH^{2+}$ and $trans-L^1RhD^{2+}$ remain unchanged as H_2O is replaced by D_2O and vice versa, Figure 3. Thus the isotopic composition of the bulk solvent and of the coordinated molecules of water in $Cr_{aq}OO^{2+}$ and $L^1\{[H(D)]_2O\}RhOO^{2+}$ is without effect.

The temperature variation in the range 2.4–25.0 °C, Table 1 and Figure 4, yielded $\Delta H_H^\ddagger = 20.3 \pm 1.8$ kJ mol⁻¹, $\Delta S_H^\ddagger = -136 \pm 6$ J mol⁻¹ K⁻¹ for $trans-L^1RhH^{2+}$ and $\Delta H_D^\ddagger = 24.7 \pm 4.3$ kJ mol⁻¹, $\Delta S_D^\ddagger = -138 \pm 15$ J mol⁻¹ K⁻¹ for $trans-L^1RhD^{2+}$.

There was no interference from the secondary catalytic steps in any of the $Cr_{aq}OO^{2+}$ reactions. For $L = L^1$, the catalytic step of eq 12 is too slow (0.4 $M^{-1} s^{-1}$) to interfere. For $L = (NH_3)_4$, the secondary reaction of eq 14 is still slow but not negligible in comparison with the reaction of interest. It is important to note that the second-order rate constants for the stoichiometric and catalytic processes are not directly comparable. In the calculation of the pseudo-first-order rate constants $k_{\psi(st)}$ and $k_{\psi(cat)}$, the multiplier changes from $[LRhH^{2+}]$ (excess reagent) to $[LRhOO^{2+}]$ (catalyst), respectively. For this reason $k_{\psi(cat)}$ is usually much smaller than $k_{\psi(st)}$. On the other hand,

**Figure 4.** Eyring plots for the reactions between $Cr_{aq}OO^{2+}$ and $trans-L^1RhH^{2+}$ and L^1RhD^{2+} .

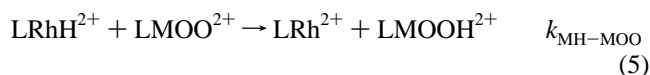
much larger quantities of product are formed in the catalytic step than in the stoichiometric reaction. This can lead to a distortion of the kinetic traces for the determination of $k_{\psi(st)}$, unless the absorbance changes for the catalytic step are negligible at the monitoring wavelength.

A macrocyclic superoxochromium complex, L^1CrOO^{2+} , reacts with rhodium hydrides much more slowly than the aqua analog does. A single experiment with $(NH_3)_4RhH^{2+}$, monitored at 270 nm, yielded $k \sim 3$ $M^{-1} s^{-1}$. There was no reaction between 0.28 mM L^1CrOO^{2+} and 0.6 mM $trans-L^1RhH^{2+}$ in 2 min, which places the rate constant at <1 $M^{-1} s^{-1}$.

The $(NH_3)_4RhOO^{2+}/trans-L^1RhH^{2+}$ reaction, eq 11, and all the other reactions between rhodium hydrides and superoxorhodium complexes are accompanied by only minor absorbance changes at 270 nm. The kinetics were monitored at 240 nm, where all the hydroperoxorhodium complexes have large but similar molar absorptivities. As a result, the secondary catalytic step interfered seriously in most cases, as shown in Figure S3²⁹ for the reaction between $trans-L^1RhH^{2+}$ and $(NH_3)_4RhOO^{2+}$. The catalytic stage takes several hours for completion, which made it possible to treat the initial portion of the trace (<500 s) as a sum of first- and zeroth-order reactions, yielding $k_{11} = 22.8$ $M^{-1} s^{-1}$.

The other combination, $trans-L^1RhOO^{2+}/(NH_3)_4RhH^{2+}$, did not produce useful kinetic data in the presence of O_2 , because the catalytic step dominates throughout. The rate constant was obtained under air-free conditions, as described below.

Kinetics under Air-Free Conditions. If the chemistry under O_2 indeed proceeds as postulated in eqs 5 and 6, then it should be possible to determine the kinetics in the absence of O_2 as well. In such circumstances the superoxo complex $LMOO^{2+}$ is the most likely candidate to take over as a scavenger for LRh^{2+} , as shown in Scheme 1. The expected rate law differs from that obtained in the presence of O_2 by a stoichiometric factor $n + 1$.

Scheme 1

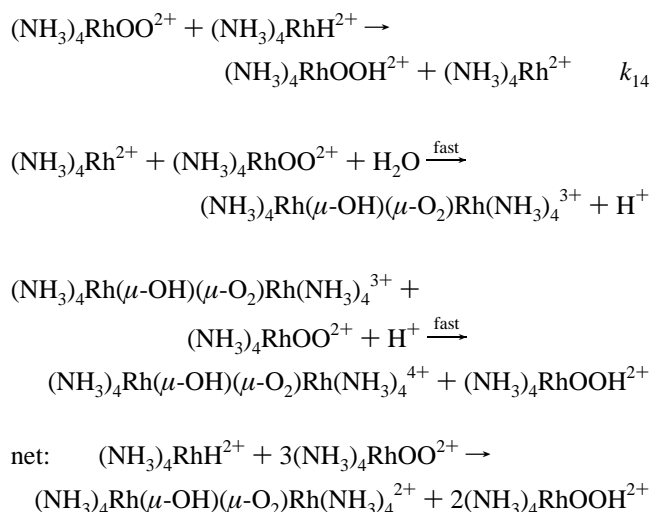
$$-d[LMOO^{2+}]/dt = (n + 1)k_{MH-MOO}[LRhH^{2+}][LMOO^{2+}]$$

The $(NH_3)_4RhOO^{2+}/(NH_3)_4RhH^{2+}$ reaction was used as a test case. The kinetic traces showed an absorbance increase at 240 nm, followed by a much slower decrease. The rate constants for the two stages were obtained from the fit to a biexponential

rate expression. Only the kinetics of the first stage were proportional to the concentration of $(\text{NH}_3)_4\text{RhH}^{2+}$, Figure 2, yielding $(n + 1)k_{14} = 93.8 \pm 4.4 \text{ M}^{-1} \text{ s}^{-1}$. The slow decreasing portion of the trace was probably caused by a switch from $(\text{NH}_3)_4\text{RhOO}^{2+}$ to reaction products, $(\text{NH}_3)_4\text{RhOOH}^{2+}$ and/or $(\text{NH}_3)_4\text{Rh}(\mu\text{-OH})(\mu\text{-O}_2)\text{Rh}(\text{NH}_3)_4^{4+}$, as scavengers for $(\text{NH}_3)_4\text{Rh}^{2+}$ in the final stages of the reaction.

The ratio of the rate constants in the absence and presence of O_2 has a value $n + 1 = 2.9 \pm 0.2$. The UV-visible spectra of spent reaction solutions exhibited bands at 360 and 560 nm, indicative of $(\text{NH}_3)_4\text{Rh}(\mu\text{-OH})(\mu\text{-O}_2)\text{Rh}(\text{NH}_3)_4^{4+}$,^{21,30} together with some $(\text{NH}_3)_4\text{Rh}^{3+}$. The nature of the product provides an independent confirmation of the stoichiometric factor $n + 1 = 3$. Scheme 2 accounts for all the observations.

Scheme 2



The reaction between *trans*- $\text{L}^1\text{RhOO}^{2+}$ and $(\text{NH}_3)_4\text{RhH}^{2+}$ under argon behaved similarly and yielded $(n + 1)k = 27.7 \pm 0.7 \text{ M}^{-1} \text{ s}^{-1}$, Figure S 2.²⁹ Assuming that the stoichiometric factor $n + 1$ is again 3, the rate constant for hydrogen atom abstraction is $9 \text{ M}^{-1} \text{ s}^{-1}$. The small value of this rate constant relative to k_{14} ($32.7 \text{ M}^{-1} \text{ s}^{-1}$) explains the observed dominance of the catalytic component (reaction 14) when *trans*- $\text{L}^1\text{RhOO}^{2+}$ / $(\text{NH}_3)_4\text{RhH}^{2+}$ reaction was conducted in the presence of O_2 .

Kinetics of the $\text{LRh}^{2+}\text{-O}_2$ Reaction. Single-shot laser-flash photolysis of 0.1–0.2 mM LRhH^{2+} in 0.01 M HClO_4 produced 3–5 μM LRh^{2+} . The ensuing reaction with O_2 to form LRhOO^{2+} caused the absorbance at 270 nm to increase. The observed pseudo-first-order rate constants for $\text{L}^1\text{Rh}^{2+}/\text{O}_2$ reaction had values $k_p = (5.1 \pm 0.2) \times 10^4 \text{ s}^{-1}$ (air-saturated) and $(2.7 \pm 0.1) \times 10^5 \text{ s}^{-1}$ (O_2 -saturated), yielding $k_{\text{on}} = (2.1 \pm 0.1) \times 10^8 \text{ M}^{-1} \text{ s}^{-1}$ (see eq 10) at 25 °C. For the reaction of L^2Rh^{2+} with O_2 , similar experiments yielded $k_{\text{on}} = (8.2 \pm 0.1) \times 10^7 \text{ M}^{-1} \text{ s}^{-1}$. Both values are somewhat smaller than that measured previously for $(\text{NH}_3)_4\text{Rh}^{2+}$ ($3.1 \times 10^8 \text{ M}^{-1} \text{ s}^{-1}$).²²

Discussion

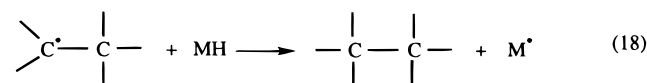
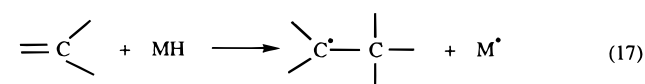
The data obtained in this work provide strong evidence for hydrogen atom transfer between superoxo and hydrido complexes. The products, metal hydroperoxides in the presence of O_2 and binuclear superoxorhodium complexes under argon, are most readily explained by invoking LRh^{2+} as an intermediate, eqs 5 and 6 and Scheme 1. Consistent with this proposal is the

observed change in the stoichiometric ratio $[\text{LMOO}^{2+}]/[\text{LRhH}^{2+}]$ from = 1:1 under O_2 to 3:1 under argon.³¹

The large deuterium isotope effects for the two cases in Table 1 clearly show the importance of the Rh–H bond cleavage in the activation process. The values $k_{\text{H}}/k_{\text{D}} = 7.6$ for the reaction of $\text{L}^1\text{RhH}^{2+}$ with $\text{Cr}_{\text{aq}}\text{OO}^{2+}$ and ~ 7 for the reaction between $\text{L}^1\text{RhH}^{2+}$ and $\text{L}^1\text{RhOO}^{2+}$ are significantly larger than the maximum value of 4.2 calculated from an expression for a simple three-center model.³² The large isotope effects suggest quantum mechanical tunneling. Also consistent with tunneling is the difference between the activation enthalpies³² for the reactions of $\text{Cr}_{\text{aq}}\text{OO}^{2+}$ with $\text{L}^1\text{RhH}^{2+}$ and $\text{L}^1\text{RhD}^{2+}$. The value, $\Delta(\Delta H^\ddagger) = \Delta H_{\text{D}}^\ddagger - \Delta H_{\text{H}}^\ddagger = 4.4 \text{ kJ/mol}$, exceeds the difference in zero-point vibrational energies, 3.6 kJ/mol, calculated from the IR data.²⁰ The weight of this argument is diminished, however, by the large standard deviations on activation parameters, including enthalpies of activation. The large deviations result from a combination of small temperature effect on reaction rates, Table 1, and a narrow temperature range used. The experimental temperature limits were determined by the melting point of the solvent on one end and the stability of the reactants and products on the other.

Other criteria used to establish tunneling, the nonlinearity of Eyring plots and the ratio of Arrhenius preexponential factors,³² are inherently less precise than the activation enthalpies, and a detailed analysis of these parameters has not been attempted. On the basis of the arguments presented, however, it appears reasonable to suggest that tunneling plays a role in hydrogen transfer between *trans*- $\text{L}^1\text{RhH}^{2+}$ and $\text{Cr}_{\text{aq}}\text{OO}^{2+}$ and probably in other reactions in Table 1 as well.

Normal kinetic isotope effects have been observed^{33,34} in hydrogen atom transfer between metal hydrides and carbon-centered radicals.³⁵ Such reactions are involved, for example, in the hydrogenation of olefins, eqs 17 and 18, and often followed by dimerization of M^\bullet . Interestingly, hydrogen atom transfer to olefin in the first step, eq 17, often occurs with an inverse isotope effect.^{33,34}



Another interesting feature of olefin hydrogenation concerns the reactivity patterns in the two steps. The energy of the metal-hydrogen bond is decisive in reaction 17,³⁵ and steric factors³⁶ are important in reaction 18. In this respect, hydrogen transfer from LRhH^{2+} to LMOO^{2+} clearly resembles reaction 18. As shown in Table 1, the rate constants for the reactions of *cis*- $\text{L}^1\text{RhH}^{2+}$, *trans*- $\text{L}^1\text{RhH}^{2+}$, and $(\text{NH}_3)_4\text{RhH}^{2+}$ with $\text{Cr}_{\text{aq}}\text{OO}^{2+}$ are

(31) Equations 5 and 6 represent a propagating sequence of a chain reaction, and the catalytic behavior is seen only as a result of special circumstances, i.e. when $\text{LRh} = \text{LM}$. A fine, but distinct, line divides the two situations: In a catalytic reaction, a molecule of catalyst enters the reaction and exits at the end. In the chain reaction of eqs 5 and 6, the LRhOO^{2+} that appears at the end is derived from LRhH^{2+} , whereas the original LRhOO^{2+} becomes the product LRhOOH^{2+} .

(32) Saunders, W. H., Jr. In *Techniques of Chemistry. Volume VI. Investigation of Rates and Mechanisms of Reactions. Part 1*; Bernasconi, C. F., Ed.; Wiley: New York, 1986; Chapter 8.

(33) Bullock, R. M. in *Transition Metal Hydrides*; Dedieu, A., Ed.; VCH: New York, 1992; pp 263–307.

(34) Bullock, R. M. *Comments Inorg. Chem.* **1991**, *12*, 1.

(35) Bullock, R. M.; Samsel, E. G. *J. Am. Chem. Soc.* **1990**, *112*, 6886.

(36) Eisenberg, D. C.; Lawrie, C. J. C.; Moody, A. E.; Norton, J. R. *J. Am. Chem. Soc.* **1991**, *113*, 4888.

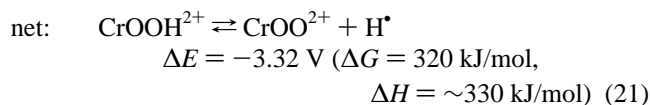
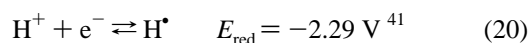
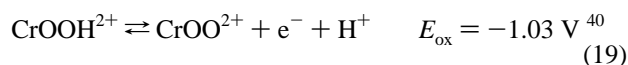
(30) Johnston, L. E.; Page, J. A. *Can. J. Chem.* **1969**, *47*, 4241.

within the error identical with each other. The reason probably lies not only in the similar steric and electronic properties of these complexes, but also in the long, three-atom bridge ($-\text{H}\cdots\text{OO}-$) in the transition state which keeps the metal centers far apart and eliminates the effect of minor steric differences. Strikingly, the isotopic substitution ($\text{L}^1\text{RhH}^{2+}$ vs $\text{L}^1\text{RhD}^{2+}$) influences the rate much more than the change of N_4 ligands from *cis* to *trans* and from a macrocycle to four ammonias.

The complex $(\text{NH}_3)_4\text{RhOO}^{2+}$ also has comparable rate constants for reactions with the two hydrides studied, $(\text{NH}_3)_4\text{RhH}^{2+}$ ($32.7 \text{ M}^{-1} \text{ s}^{-1}$) and $\text{L}^1\text{RhH}^{2+}$ ($22.8 \text{ M}^{-1} \text{ s}^{-1}$). The values are smaller than those for the equivalent reactions with $\text{Cr}_{\text{aq}}\text{OO}^{2+}$ by a factor of ~ 5 . It is tempting to suggest that this factor arises mainly from the difference in $\text{Cr}_{\text{aq}}\text{OO}-\text{H}^{2+}$ and $(\text{NH}_3)_4\text{RhOO}-\text{H}^{2+}$ bond energies, but such conclusions may be premature in view of the large number of parameters that determine the activation energies for hydrogen transfer.^{37,38}

In keeping with the steric argument, the more crowded $\text{L}^2\text{RhH}^{2+}$ reacts with $\text{Cr}_{\text{aq}}\text{OO}^{2+}$ more slowly than *trans*- $\text{L}^1\text{RhH}^{2+}$ does, although different thermodynamic stabilities for $\text{L}^1\text{RhH}^{2+}$ and $\text{L}^2\text{RhH}^{2+}$ cannot be ruled out entirely as the source of kinetic differences. A major drop in rates is observed in all the reactions taking place between two macrocyclic complexes, where nonbonding interactions in the transition state are expected to be the greatest.

The rapid scavenging of the rhodium(II) product by O_2 or LMOO^{2+} makes all the reactions in Table 1 irreversible, so that the kinetic data provide no information on thermodynamics. On the basis of limited data for the appropriate O–H and Rh–H bond energies, it does seem likely that the reactions in Table 1 are thermodynamically favorable. The energy of the $\text{Cr}_{\text{aq}}\text{OO}-\text{H}^{2+}$ bond can be estimated from the thermochemical scheme in eqs 19–21. Under the assumption that the entropies of $\text{Cr}_{\text{aq}}\text{OOH}^{2+}$ and $\text{Cr}_{\text{aq}}\text{OO}^{2+}$ are comparable, the ΔS^0 for reaction 21 is determined by S^0 for $\text{H}_{\text{aq}}^{\bullet}$ (38 J/mol K),³⁹ yielding $\Delta H^0 = \text{BDE} \sim 330 \text{ kJ/mol}$, significantly smaller than BDE's for $\text{HOO}-\text{H}$ and $\text{ROO}-\text{H}$ (369 kJ/mol).³⁸



The energy of the Rh–H bonds in LRhH^{2+} complexes is more difficult to estimate. Even though bond energies for a large number of transition metal hydrides are available,^{34,41–49} the information on rhodium hydrides is limited,⁴² and there are no data for cationic complexes. The estimates of BDE's for

$(\text{oep})\text{Rh}-\text{H}$ (259 kJ/mol),^{50,51} $(\text{tmp})\text{Rh}-\text{H}$ (~ 250),^{50,51} $(\text{txp})\text{Rh}-\text{H}$ (~ 250),^{50,51} and $(\text{dbpb})\text{Rh}-\text{H}$ ("comparable to those for rhodium porphyrin complexes")^{46,50} and the mean BDE for $\text{RhCl}[\text{P}(4\text{-tolyl})_3]_3(\text{H})_2$ (241)⁵² and $\text{RhCl}(\text{thtp})[\text{P}(4\text{-tolyl})_3]_2(\text{H})_2$ (242)^{50,52} are all within $< 20 \text{ kJ/mol}$, demonstrating the modest role of ligands in determining the Rh–H bond energy. The change to the dicationic LRhH^{2+} is bound to have some effect, but even if one allows the BDE of $\text{LRh}-\text{H}^{2+}$ to exceed the average known BDE of rhodium(III) hydrides by a generous 20 kJ/mol , the energy of $\text{LRh}-\text{H}^{2+}$ bond ($\leq 270 \text{ kJ/mol}$) would still be much lower than the energy of the O–H bond in $\text{Cr}_{\text{aq}}\text{OOH}^{2+}$ ($\sim 330 \text{ kJ/mol}$), creating a sizable driving force for hydrogen transfer.

Our results clearly show that superoxometal complexes can and do engage in hydrogen atom transfer. The activation energy, at least for the reaction between $\text{Cr}_{\text{aq}}\text{OO}^{2+}$ and $\text{L}^1\text{RhH}^{2+}$, is small, and major contribution to the activation barrier comes from the ΔS^\ddagger term. Large negative entropies of activation are to be expected for bimolecular reactions between species of equal charge, although the magnitude of the ΔS^\ddagger term for $\text{Cr}_{\text{aq}}\text{OO}^{2+}/\text{L}^1\text{RhH}^{2+}$ reaction (-136 J/mol K) does seem somewhat larger than usual. Along the same lines, the sensitivity of the reaction to steric effects is large for the reactions in Table 1, where three intervening atoms separate the two metal centers in the activated complex. In catalytic oxidations of organic materials, the driving force for hydrogen atom abstraction by superoxometal complexes is smaller than in the reactions in Table 1. The less favorable energetics combined with the pronounced sensitivity to steric congestion may be the reason that superoxometal intermediates seem to react preferentially by pathways other than hydrogen transfer.

Acknowledgment. Thanks are due to Dr. Espenson and Dr. Angelici for useful discussions and comments, Dr. W.-D. Wang for help with some experiments, Dr. S. Bajic for his help in obtaining the IR spectra, and the reviewers for helpful comments. This work was supported by the U.S. Department of Energy, Office of Basic Energy Sciences, Division of Chemical Sciences, under Contract W-7405-Eng-82.

Supporting Information Available: UV–visible spectra of reactants and products of $\text{L}^1\text{RhH}^{2+}/\text{Cr}_{\text{aq}}\text{OO}^{2+}$ reaction, a plot of k_{obs} vs $[(\text{NH}_3)_4\text{RhH}^{2+}]$ for the $(\text{NH}_3)_4\text{RhH}^{2+}/(\text{NH}_3)_4\text{RhOO}^{2+}$ reaction under argon, and a kinetic trace for the $\text{L}^1\text{RhH}^{2+}/(\text{NH}_3)_4\text{RhOO}^{2+}$ reaction (4 pages). See any current masthead page for ordering and Internet access instructions.

JA971987G

(43) Pearson, R. G. In *Bonding Energetics in Organometallic Compounds*; Marks, T. J., Ed.; American Chemical Society: Washington, DC, 1990; pp 251–262.

(44) Pearson, R. G. *Chem. Rev.* **1985**, *85*, 41.

(45) Wang, D.; Angelici, R. J. *J. Am. Chem. Soc.* **1996**, *118*, 935.

(46) Wei, M.; Wayland, B. B. *Organometallics* **1996**, *15*, 4681.

(47) Parker, V. D.; Handoo, K. L.; Roness, F.; Tilset, M. *J. Am. Chem. Soc.* **1991**, *113*, 7493.

(48) Skagestad, V.; Tilset, M. *J. Am. Chem. Soc.* **1993**, *115*, 5077.

(49) Tilset, M. *J. Am. Chem. Soc.* **1992**, *114*, 2740.

(50) Abbreviations: oep = octaethylporphyrinate dianion; tmp = tetramesitylporphyrinate dianion; txp = tetraxylylporphyrinate dianion; dbpb = 4,5-dimethyl-1,2-bis(4-(1-butylpentyl)pyridine-2-carboxamido)benzene dianion; thtp = tetrahydrothiophene.

(51) Wayland, B. B.; Ba, S.; Sherry, A. E. *J. Am. Chem. Soc.* **1991**, *113*, 5305.

(52) Drago, R. S.; Miller, J. G.; Hoselton, M. A.; Farris, R. D.; Desmond, M. J. *J. Am. Chem. Soc.* **1983**, *105*, 444.

(37) Roberts, B. P. *J. Chem. Soc., Perkin Trans. 2* **1996**, 2719.

(38) Zavitsas, A. A.; Chatgillaloglu, C. *J. Am. Chem. Soc.* **1995**, *117*, 10645.

(39) Buxton, G. V.; Greenstock, C. L.; Helman, W. P.; Ross, A. B. *J. Phys. Chem. Ref. Data* **1988**, *17*, 513.

(40) Kang, C.; Anson, F. C. *Inorg. Chem.* **1994**, *33*, 2624.

(41) Wayner, D. D. M.; Parker, V. D. *Acc. Chem. Res.* **1993**, *26*, 287.

(42) Simoes, J. A. M.; Beauchamp, J. L. *Chem. Rev.* **1990**, *90*, 629.